

## The Space Density Evolution of Wet and Dry Mergers in the Canada-France-Hawaii Telescope Legacy Survey

Richard C. Y. Chou,<sup>1</sup> Carrie R. Bridge,<sup>2</sup> and Roberto G. Abraham<sup>3</sup>

<sup>1</sup>*Department of Astronomy and Astrophysics, University of Toronto, 50 St. George Street, Toronto, ON M5S 3H4; chou@astro.utoronto.ca*

<sup>2</sup>*California Institute of Technology, 1200 East California Blvd. 91125; bridge@astro.caltech.edu* <sup>3</sup>*Department of Astronomy and Astrophysics, University of Toronto, 50 St. George Street, Toronto, ON M5S 3H4; abraham@astro.utoronto.ca*

### Abstract.

We analyze 1298 merging galaxies with redshifts up to  $z = 0.7$  from the Canada-France-Hawaii Telescope Legacy Survey, taken from the catalog presented in Bridge et al. (2010). By analyzing the internal colors of these systems, we show that so-called wet and dry mergers evolve in different senses, and quantify the space densities of these systems. The local space density of wet mergers is essentially identical to the local space density of dry mergers. The evolution in the total merger rate is modest out to  $z \sim 0.7$ , although the wet and dry populations have different evolutionary trends. At higher redshifts dry mergers make a smaller contribution to the total merging galaxy population, but this is offset by a roughly equivalent increase in the contribution from wet mergers. By comparing the mass density function of early-type galaxies to the corresponding mass density function for merging systems, we show that not all the major mergers with the highest masses ( $M_{\text{stellar}} > 10^{11} M_{\odot}$ ) will end up with the most massive early-type galaxies, unless the merging timescale is dramatically longer than that usually assumed. On the other hand, the usually-assumed merging timescale of  $\sim 0.5-1$  Gyr is quite consistent with the data if we suppose that only less massive early-type galaxies form via mergers. Since low-intermediate mass ellipticals are 10–100 times more common than their most massive counterparts, the hierarchical explanation for the origin of early-type galaxies may be correct for the vast majority of early-types, even if incorrect for the most massive ones.

## 1. INTRODUCTION

Galaxy mergers are essential building blocks under the hierarchical galaxy formation scenario. Conventionally people use a power law  $(1+z)^m$  to parametrize the merger rate. Despite the effort that has been dedicated to constrain the power law index  $m$  in the past decade (Bundy et al. 2009; Conselice et al. 2003; Bridge et al. 2007; Lin et al. 2008; Lotz et al. 2008; Jogee et al. 2009), however, the evolution of merger rate still remains elusive. A recent study by Bridge et al. (2010) analyzed these published merger rates and concluded that, overall, there is a general agreement that the merger rate at intermediate redshifts ( $0.2 < z < 1.2$ ) does evolve, although the constraints on  $m$  remain fairly mild. Bridge et al. (2010) rule out  $m < 1.5$  (i.e. flat or mild evolution)

and suggest that the wide range of  $m$  reported in the literature is due to a combination of factors, including variation in the redshift ranges being probed, small sample sizes in some of the surveys, and cosmic variance.

In this paper, we implemented the best pattern recognizer - the brain-eye combination to select mergers. Second, instead of using the traditional merger fractions to describe the merger evolution, we use the space density corrected by the standard  $1/V_{\max}$  formalism (Felten 1977; Schmidt 1968) to provide a luminosity bias free and more physical meaning picture for the merger evolution.

An important subsidiary goal of the present paper is to chart the differential merging history of color-selected sub-classes of merging galaxies. In recent years a host of observations have shown the evolutionary histories of galaxies in the so-called ‘red sequence’ and ‘blue cloud’ are different (Bundy et al. 2009; de Ravel et al. 2009; Lin et al. 2008; Willmer et al. 2006). This has led to the idea that it is important to distinguish between mergers that result in significant star-formation (‘wet mergers’) and those which merely re-organize existing stellar populations (‘dry mergers’). However, the importance of these wet and dry mergers in the formation of red sequence galaxies is still not clear (Bell et al. 2007; Bundy et al. 2004, 2009; Faber et al. 2007; Lin et al. 2008; Scarlata et al. 2007), and it is of interest to determine if wet and dry merging systems exhibit similar evolutionary trends as a function of cosmic epoch.

Throughout this paper, we adopt a concordance cosmology with  $H_0=70 \text{ km s}^{-1}\text{Mpc}^{-1}$ ,  $\Omega_M = 0.3$ , and  $\Omega_\Lambda = 0.7$ . All photometric magnitudes are given in the AB system.

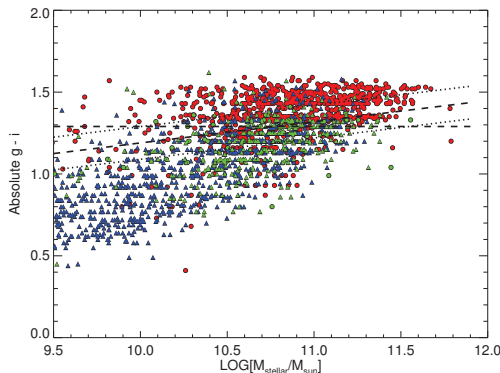


Figure 1.  $g' - i'$  rest frame color versus stellar mass in log unit of  $\sim 2200$  field galaxies in the CFHTLS survey used for merger color classification. See text for details.

## 2. OBSERVATIONS

As has already been noted, a detailed description of the selection strategy for (and basic properties of) the galaxies analyzed in the present paper has already been presented in Bridge et al. (2010). The reader is referred to that paper for details beyond the outline presented here.

## 2.1. Data

The data in this paper come from two of the Canada-France-Hawaii Telescope Legacy Survey (CFHTLS) deep survey fields. These fields (denoted D1 and D2) together cover an area of 2 square degrees. The CFHTLS deep survey has high-quality broad-band photometry in five bands ( $u^*$ ,  $g'$ ,  $r'$ ,  $i'$ ,  $z'$ ) and the depth of the survey ranges from 26.0 ( $z'$ ) to 27.8 ( $g'$ ). The typical seeing for the final stacks is  $0.7''$ - $0.8''$  in the  $i'$ -band.

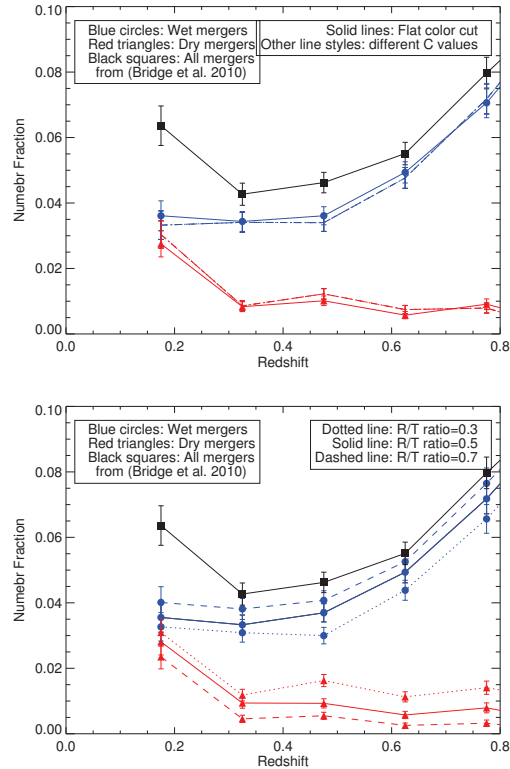


Figure 2. Merger fractions computed using two different methods. Red and blue curves represent the merger fractions of dry and wet mergers. [Left] Merger fraction derived from different fiducial color cuts with integrated colors in different line styles (i.e., different  $C$  values in equation (1)). [Right] Merger fractions derived from different internal color ratios.

## 2.2. Merger identifications

Merging galaxies were selected visually, with multiple cross-checks on the visual classifications, and using simulations to characterize detection thresholds for features that are signatures of mergers. Interacting galaxies are defined as systems with a tidal tail or bridge. All galaxies down to an  $i'_{vega} \leq 22.9$  mag ( $\sim 27,000$ ) were inspected resulting in a final sample of 1298 merging galaxies. The merger identification rate for galaxies with  $i'_{vega} \leq 21.9$  mag is estimated to be  $> 90\%$ , and is used as the limit for merger identification. A group of galaxy mergers with redshift ranges from  $z = 0.3$  to  $z = 0.45$

and  $M_g \leq -21.0$  mag were selected to estimate the detection completeness. They were artificially redshifted to higher redshifts after accounting for the k-correction, change in angular size and surface brightness dimming. After this step the merger identification was conducted again and  $\sim 85\%$  of the redshifted mergers was classified as mergers up to  $z = 0.7$ . This redshift limit is also used as the upper limit when performing the  $1/V_{\max}$  correction to eliminate the Malmquist bias and compute space densities. *It is important to note that  $V_{\max}$  of mergers presented in this paper is defined as the maximum volume over which mergers can be identified as such, and not the maximum redshift at which a given galaxy's integrated magnitude remains above the detection threshold.*

### 2.3. Galaxy properties

The galaxy properties were derived by comparing the spectral energy distributions (SEDs) obtained from observed fluxes to a set of template SEDs. The best-fit SEDs were determined through a standard minimum  $\chi^2$  fitting between the template SEDs and the observed fluxes. The template SEDs were computed by the PEGASE-II galaxy evolution code (Le Borgne et al. 2004) and were integrated through the CFHT filters. The SED fits were undertaken using the Z-Peg code (Le Borgne & Rocca-Volmerange 2002) and details are described in Bridge et al. (2010). The photometric accuracy is determined by comparing the derived photometric redshifts to the spectroscopic redshifts in the SNLS sample (Bronder et al. 2008). The accuracy of the photometric redshift down to  $i \sim 22.5$  is  $\sigma_{\Delta z}/(1+z) = 0.04$ .

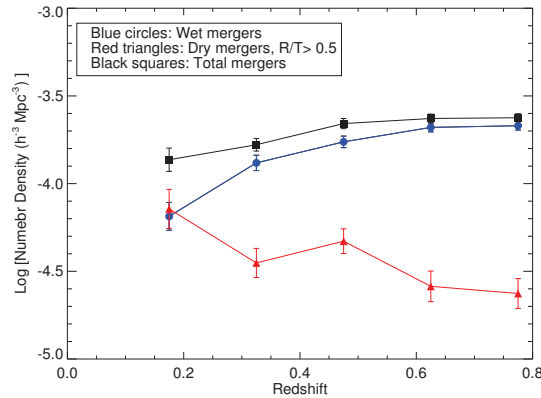


Figure 3. Space densities of wet and dry mergers. See text for details.

### 3. Classification of Wet and Dry Mergers

We divide galaxies into ‘red’ and ‘blue’ categories utilizing the so called ‘color bimodality’ method. The fiducial color is defined by using the  $\sim 2200$  visually classified field galaxies in CFHTLS D1 and D2 field on the rest-frame  $g' - i'$  versus galaxy stellar mass diagram (see Figure 1). Red dots represent visually classified elliptical galaxies and blue dots indicate spiral galaxies. The green dots indicate the objects with MIPS  $24\mu\text{m}$  detection (down to a flux limit of  $340 \mu\text{Jy}$ ). Cowie & Barger (2008) report that

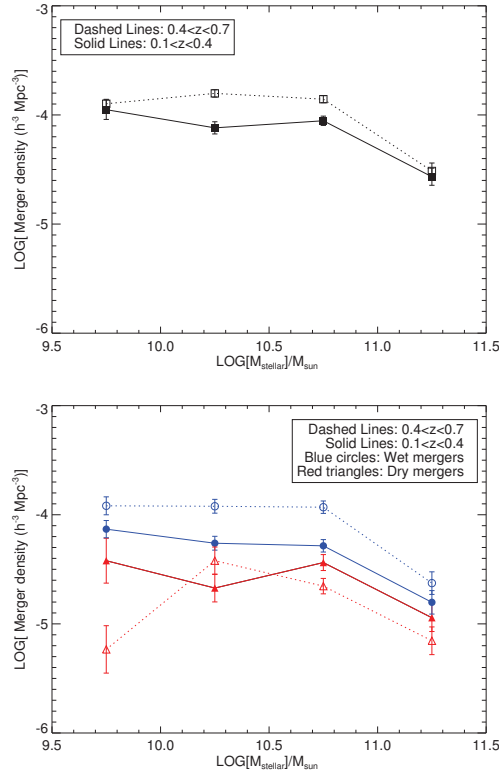


Figure 4. [Left] Mass density functions of total mergers in two redshift bins. [Right] Mass density functions of wet and dry mergers in blue and red curves.

at  $z < 1.5$  most red galaxies with a  $24\mu\text{m}$  flux  $> 80\mu\text{Jy}$  fall into the blue cloud after the appropriate dust extinction is applied. Thus, we artificially assign the green dots with  $g' - i'$  color greater than the color bimodality to the blue cloud. The stellar-mass-dependent fiducial color cut was adopted based on the red sequence fitting of 115 visually classified elliptical field galaxies with spectroscopic redshifts from Cosmological Evolution Survey (COSMOS) (Scoville et al. 2007; Lilly et al. 2007). The fitting line is expressed by the following equation:

$$(g' - i')_{\text{rest}} = -0.0076 + 0.13 \times M_{\text{stellar}} - C \quad (1)$$

The constant  $C$  serves as a parameter to control the vertical position of the fitting line on the diagram. To account for the potential classification errors caused by different slopes and  $C$  values, we have explored the implications of changing the free parameters in Equation (1). In addition, we also perform the color classification with a flat color cut  $g' - i' = 1.29$  that has the same amount of red (blue) galaxy contamination in blue (red) clouds. As a result, we find that all trends reported in this paper remain robust to the specific numerical values chosen (see Fig. 2 for details).

### 3.1. Methods

The first method for segregating wet mergers from dry mergers is to look at the total integrated  $g' - i'$  color of the merger. Mergers whose integrated colors are redder than the threshold are deemed ‘dry’, and systems bluer than the threshold are deemed ‘wet’. The second method is based on analysis of the colors of individual pixels to avoid non-uniform color distribution problem that the integrated color method may encounter. Pixels with rest-frame  $g' - i'$  color greater than the fiducial threshold are labeled as ‘red’, and the ratio of the total flux in red pixels to the flux in all pixels is calculated. We refer to this quantity as the ‘Red-to-Total ratio’,  $(R/T)$ , given by:

$$(R/T) = \frac{F_{red}}{F_{total}} \quad (2)$$

where  $F_{red}$  indicates flux contained in red pixels and  $F_{total}$  refers to the flux from the entire merger.

## 4. RESULTS

### 4.1. Merger Fractions

Merger fractions were computed using the integrated color and internal color methods, result is shown in Figure 2. Red and blue curves represent the merger fractions of dry and wet mergers. Figure 2 left panel shows the merger fraction derived from different fiducial color cuts with integrated colors in different line styles (i.e., different  $C$  values in equation (1)). Figure 2 right panel shows the merger fractions derived from different internal color ratios. In both panels, red curves indicate dry mergers, blue curves indicate wet mergers, and black curves indicate the total merging population. Error bars are estimated by assuming Poisson errors. In the left panel, different color cuts do not affect the scientific results, and in the right panel different red to total ratios also do not change the overall merger fraction evolution trend, showing the result is robust under different wet and dry merger classification conditions. Since the result from the integrated color method is consistent with that from  $R/T$  equals to 0.5, we fix  $R/T = 0.5$  as the threshold in classifying wet and dry mergers for the following results. If parametrize the curve with  $R/T = 0.5$  with the power law  $(1 + z)^m$ , we obtained  $m = 0.2 \pm 0.3$  and  $m = -3.1 \pm 0.5$  for wet and dry mergers, respectively.

### 4.2. The Space Density of Merging Galaxies

Figure 3 shows the space density of wet and dry mergers in CFHTLS. Blue and red curves correspond to wet and dry mergers, respectively, while the black curve shows the total for all mergers. These space densities were computed by weighting each merger by  $1/V_{max}$  and summing over redshift bins. The growth in the total space density of mergers is modest, increasing by about a factor of two over the redshift range probed. The wet and dry merging galaxies show opposite trends with redshift. The space density of wet mergers is increasing with redshift, while that of dry mergers is (perhaps) modestly decreasing. Note that the space density of dry mergers becomes important in the relatively low redshift range and crossover with that of wet mergers at  $z \sim 0.2$ .

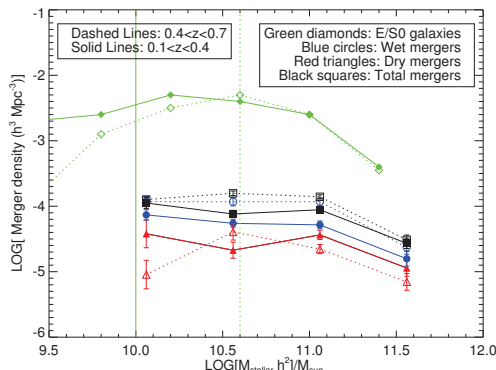


Figure 5. A comparison of mass density functions between galaxy mergers and early type galaxies taken from Bundy et al. 2004.

### 4.3. The Stellar Mass Density Function

Figure 4 left panel shows the mass density functions of total mergers in two redshift bins. The high-redshift bin ( $0.4 < z < 0.7$ ) is shown with a dashed curve, while the low redshift bin ( $0.1 < z < 0.4$ ) is shown with a solid curve. We see evidence for modest evolution in the mass density function, with most change occurring at intermediate masses, and no change at the high and low mass ends. Figure 4 right panel shows the mass density functions of wet and dry mergers in blue and red curves. Different line styles segregate the data into two redshift bins, as for the left-hand panel. For mergers in the most massive bin, an increase in the dry merger space density is offset by a decrease in the wet merger space density, so the total space density is nearly conserved. At intermediate masses, the mass density function of dry mergers is nearly unchanged in both redshift bins, with perhaps some evidence for a slight decrease in the space density of intermediate-mass dry mergers at high redshifts. On the other hand, the mass density function of wet mergers is increasing with redshift.

## 5. DISCUSSION

Figure 5 shows a comparison of the stellar mass density function for mergers in the present sample with the corresponding stellar mass density function for early-type galaxies presented in Bundy et al. (2005). The data point of early type galaxies are more or less from the same redshift bins. Two vertical lines indicate the completeness limit of early type galaxies in different redshifts. First of all, the shapes for mergers and early type galaxies are completely different. Given a relatively flat merger space density evolution history mentioned above and assuming a constant merging timescale, one should expect that that mass density function of early type galaxies should have the same shape as that of mergers but with higher number densities. The different shape in mass density functions of both early type galaxies and mergers implies that there is no 1:1 relation between these two groups, unless the merging timescale is a strong function of stellar mass. Second, the number density of early type galaxies can be estimated by using the space density of mergers and assuming a certain merging timescale. That

is,  $N_{\text{early}} = N_{\text{merger}} \times \frac{T}{t_m}$ , here we approximate the merger space density as a constant over a cosmic timescale of six billion years (for redshift up to  $z \sim 0.7$ ) and adopt a typical merging timescale  $t_m = 0.8$ . We discover that the predicted number density of early type galaxies at the highest mass bin exceeds the actual number density of early type galaxies. That is, *not all massive mergers would end up with massive early type galaxies, unless the merging timescale is longer than the expected value*. For mergers in lower mass bins, galaxy mergers contribute  $\sim 30\%$  -  $50\%$  of early type galaxies presented in the low redshift Universe.

## References

- Bell, E. F., Zheng, X. Z., Papovich, C., Borch, A., Wolf, C., & Meisenheimer, K. 2007, ApJ, 663, 834. [0704.3077](#)
- Bridge, C. R., Appleton, P. N., Conselice, C. J., Choi, P. I., Armus, L., Fadda, D., Laine, S., Marleau, F. R., Carlberg, R. G., Helou, G., & Yan, L. 2007, ApJ, 659, 931. [arXiv:astro-ph/0701040](#)
- Bridge, C. R., Carlberg, R. G., & Sullivan, M. 2010, ApJ, 709, 1067. [1001.2772](#)
- Bronder, T. J., Hook, I. M., Astier, P., Balam, D., Balland, C., Basa, S., Carlberg, R. G., Conley, A., Fouchez, D., Guy, J., Howell, D. A., Neill, J. D., Pain, R., Perrett, K., Pritchett, C. J., Regnault, N., Sullivan, M., Baumont, S., Fabbro, S., Filliol, M., Perlmutter, S., & Ripoche, P. 2008, A&A, 477, 717. [0709.0859](#)
- Bundy, K., Ellis, R. S., & Conselice, C. J. 2005, ApJ, 625, 621. [arXiv:astro-ph/0502204](#)
- Bundy, K., Fukugita, M., Ellis, R. S., Kodama, T., & Conselice, C. J. 2004, ApJ, 601, L123. [arXiv:astro-ph/0312222](#)
- Bundy, K., Fukugita, M., Ellis, R. S., Targett, T. A., Belli, S., & Kodama, T. 2009, ApJ, 697, 1369. [0902.1188](#)
- Conselice, C. J., Bershadsky, M. A., Dickinson, M., & Papovich, C. 2003, AJ, 126, 1183. [arXiv:astro-ph/0306106](#)
- Cowie, L. L., & Barger, A. J. 2008, ApJ, 686, 72. [0806.3457](#)
- de Ravel, L., Le Fèvre, O., Tresse, L., Bottini, D., Garilli, B., Le Brun, V., Maccagni, D., Scaramella, R., Scodreggio, M., Vettolani, G., Zanichelli, A., Adami, C., Arnouts, S., Bardelli, S., Bolzonella, M., Cappi, A., Charlot, S., Ciliegi, P., Contini, T., Foucaud, S., Franzetti, P., Gavignaud, I., Guzzo, L., Ilbert, O., Iovino, A., Lamareille, F., McCracken, H. J., Marano, B., Marinoni, C., Mazure, A., Meneux, B., Merighi, R., Paltani, S., Pellò, R., Pollo, A., Pozzetti, L., Radovich, M., Vergani, D., Zamorani, G., Zucca, E., Bondi, M., Bongiorno, A., Brinchmann, J., Cucciati, O., de La Torre, S., Gregorini, L., Memeo, P., Perez-Montero, E., Mellier, Y., Merluzzi, P., & Temporin, S. 2009, A&A, 498, 379. [0807.2578](#)
- Faber, S. M., Willmer, C. N. A., Wolf, C., Koo, D. C., Weiner, B. J., Newman, J. A., Im, M., Coil, A. L., Conroy, C., Cooper, M. C., Davis, M., Finkbeiner, D. P., Gerke, B. F., Gebhardt, K., Groth, E. J., Guhathakurta, P., Harker, J., Kaiser, N., Kassin, S., Kleinheinrich, M., Konidaris, N. P., Kron, R. G., Lin, L., Luppino, G., Madgwick, D. S., Meisenheimer, K., Noeske, K. G., Phillips, A. C., Sarajedini, V. L., Schiavon, R. P., Simard, L., Szalay, A. S., Vogt, N. P., & Yan, R. 2007, ApJ, 665, 265. [arXiv:astro-ph/0506044](#)
- Felten, J. E. 1977, AJ, 82, 861
- Jogee, S., Miller, S. H., Penner, K., Skelton, R. E., Conselice, C. J., Somerville, R. S., Bell, E. F., Zheng, X. Z., Rix, H., Robaina, A. R., Barazza, F. D., Barden, M., Borch, A., Beckwith, S. V. W., Caldwell, J. A. R., Peng, C. Y., Heymans, C., McIntosh, D. H., Häubler, B., Jahnke, K., Meisenheimer, K., Sanchez, S. F., Wisotzki, L., Wolf, C., & Papovich, C. 2009, ApJ, 697, 1971. [0903.3700](#)
- Le Borgne, D., & Rocca-Volmerange, B. 2002, A&A, 386, 446. [arXiv:astro-ph/0202359](#)
- Le Borgne, D., Rocca-Volmerange, B., Prugniel, P., Lançon, A., Fioc, M., & Soubiran, C. 2004, A&A, 425, 881. [arXiv:astro-ph/0408419](#)



- Lilly, S. J., Le Fèvre, O., Renzini, A., Zamorani, G., Scodreggio, M., Contini, T., Carollo, C. M., Hasinger, G., Kneib, J., Iovino, A., Le Brun, V., Maier, C., Mainieri, V., Mignoli, M., Silverman, J., Tasca, L. A. M., Bolzonella, M., Bongiorno, A., Bottini, D., Capak, P., Caputi, K., Cimatti, A., Cucciati, O., Daddi, E., Feldmann, R., Franzetti, P., Garilli, B., Guzzo, L., Ilbert, O., Kampczyk, P., Kovac, K., Lamareille, F., Leauthaud, A., Borgne, J., McCracken, H. J., Marinoni, C., Pello, R., Ricciardelli, E., Scarlata, C., Vergani, D., Sanders, D. B., Schinnerer, E., Scoville, N., Taniguchi, Y., Arnouts, S., Aussel, H., Bardelli, S., Brusa, M., Cappi, A., Ciliegi, P., Finoguenov, A., Foucaud, S., Franceschini, R., Halliday, C., Impey, C., Knobel, C., Koekemoer, A., Kurk, J., Maccagni, D., Maddox, S., Marano, B., Marconi, G., Meneux, B., Mobasher, B., Moreau, C., Peacock, J. A., Porciani, C., Pozzetti, L., Scaramella, R., Schiminovich, D., Shopbell, P., Smail, I., Thompson, D., Tresse, L., Vettolani, G., Zanichelli, A., & Zucca, E. 2007, *ApJS*, 172, 70. [arXiv:astro-ph/0612291](#)
- Lin, L., Patton, D. R., Koo, D. C., Casteels, K., Conselice, C. J., Faber, S. M., Lotz, J., Willmer, C. N. A., Hsieh, B. C., Chiueh, T., Newman, J. A., Novak, G. S., Weiner, B. J., & Cooper, M. C. 2008, *ApJ*, 681, 232. **0802.3004**
- Lotz, J. M., Davis, M., Faber, S. M., Guhathakurta, P., Gwyn, S., Huang, J., Koo, D. C., Le Floch, E., Lin, L., Newman, J., Noeske, K., Papovich, C., Willmer, C. N. A., Coil, A., Conselice, C. J., Cooper, M., Hopkins, A. M., Metevier, A., Primack, J., Rieke, G., & Weiner, B. J. 2008, *ApJ*, 672, 177. [arXiv:astro-ph/0602088](#)
- Scarlata, C., Carollo, C. M., Lilly, S. J., Feldmann, R., Kampczyk, P., Renzini, A., Cimatti, A., Halliday, C., Daddi, E., Sargent, M. T., Koekemoer, A., Scoville, N., Kneib, J., Leauthaud, A., Massey, R., Rhodes, J., Tasca, L., Capak, P., McCracken, H. J., Mobasher, B., Taniguchi, Y., Thompson, D., Ajiki, M., Aussel, H., Murayama, T., Sanders, D. B., Sasaki, S., Shioya, Y., & Takahashi, M. 2007, *ApJS*, 172, 494. [arXiv:astro-ph/0701746](#)
- Schmidt, M. 1968, *ApJ*, 151, 393
- Scoville, N., Aussel, H., Brusa, M., Capak, P., Carollo, C. M., Elvis, M., Giavalisco, M., Guzzo, L., Hasinger, G., Impey, C., Kneib, J., LeFevre, O., Lilly, S. J., Mobasher, B., Renzini, A., Rich, R. M., Sanders, D. B., Schinnerer, E., Schminovich, D., Shopbell, P., Taniguchi, Y., & Tyson, N. D. 2007, *ApJS*, 172, 1. [arXiv:astro-ph/0612305](#)
- Willmer, C. N. A., Faber, S. M., Koo, D. C., Weiner, B. J., Newman, J. A., Coil, A. L., Connolly, A. J., Conroy, C., Cooper, M. C., Davis, M., Finkbeiner, D. P., Gerke, B. F., Guhathakurta, P., Harker, J., Kaiser, N., Kassin, S., Konidaris, N. P., Lin, L., Luppino, G., Madgwick, D. S., Noeske, K. G., Phillips, A. C., & Yan, R. 2006, *ApJ*, 647, 853. [arXiv:astro-ph/0506041](#)